Narrow inhomogeneous and homogeneous optical linewidths in a rare earth doped transparent ceramic

A. Ferrier, C. W. Thiel, B. Tumino, M. O. Ramirez, L. E. Bausá, R. L. Cone, A. Ikesue, and Ph. Goldner

Phys. Rev. B **87**, 041102 — Published 11 January 2013

DOI: 10.1103/PhysRevB.87.041102

Narrow inhomogeneous and homogeneous optical linewidths in a rare earth doped transparent ceramic

A. Ferrier,[1] C. W. Thiel,[2] B. Tumino,[1] M. O. Ramirez,[3] L. E. Bausá,[3] R. L. Cone,[2] A. Ikesue,[4] and Ph. Goldner[1,*]

[1] *Chimie ParisTech, Laboratoire de Chimie de la Matière Condensée de Paris, CNRS-UMR 7574, UPMC Univ Paris 06, 11 rue Pierre et Marie Curie 75005 Paris, France*

[2] *Department of Physics, Montana State University, Bozeman, Montana 59717, USA*

[3] *Dept. Física de Materiales and Instituto Nicolás Cabrera, Universidad Autónoma de Madrid, 28049 Madrid, Spain*

[4] *World Lab., Mutsuno, Atsuta-ku, Nagoya 456-0023, Japan*

(Dated: January 3, 2013)

Inhomogeneous and homogeneous linewidth are reported in a Eu^{3+} doped transparent Y_2O_3 ceramic for the $^7F_0$-$^5D_0$ transition, using high resolution coherent spectroscopy. The 8.7 GHz inhomogeneous linewidth is close to that of single crystals, as is the 59 kHz homogeneous linewidth at 3 K ($T_2 = 5.4\ \mu s$). The homogeneous linewidth exhibits a temperature dependence that is typical of a crystalline environment, and additional dephasing observed in the ceramic is attributed to magnetic impurities or defects introduced during the synthesis process. The absence of Eu^{3+}segregation at the grain boundaries, evidenced through confocal microfluorescence, further indicates that the majority of Eu^{3+}ion in the ceramic experience an environment comparable to a single crystal. The obtained results suggest that ceramics materials can be competitive with single crystals for applications in quantum information and spectral hole burning devices, beyond their current applications in lasers and scintillators.

PACS numbers: 42.50.Md,76.30.Kg,42.70.-a,42.62.Fi

Rare earth doped transparent polycrystalline ceramics have recently attracted much attention as new laser hosts[1–3] and scintillating materials[4–6]. Compared to single crystals, they can be obtained in larger volumes and with higher doping level. Other advantages include high mechanical robustness, flexibility in shape, and ease of manufacturing composite materials or controlled composition gradients. Highly efficient laser oscillations have been reported for several materials including Nd^{3+}:$Y_3Al_5O_{12}$[7,8],Yb^{3+}:$Y_3Al_5O_{12}$[9], Yb^{3+}:Y_2O_3[10] and Er^{3+}:Y_2O_3[11], demonstrating that low optical losses can be achieved in these materials. Rare earth optical spectroscopy also revealed that absorption and emission cross-sections, as well as excited state lifetimes, can be very close to those observed in single crystals at ambient temperatures.[2] For single crystals, it is known that optical transitions of rare earth ion impurities can exhibit very narrow inhomogeneous and homogeneous linewidths due to shielding of 4f electrons by the outer 5s and 5p closed shells. This has been used recently in the field of quantum memories[12] to demonstrate storage of entangled photons[13,14], entanglement of crystals[15], and high efficiency quantum storage[16]. The narrow spectral holes that can be burned into rare earth absorption lines have also enabled continuous analysis of optically carried radio frequency signals[17], ultrasound optical tomography[18] or laser frequency stabilization[19,20]. Ceramic materials could be an alternative to single crystals in these applications, offering unique possibilities for flexible shaping and composition, but only if the rare earth linewidths, especially the homogeneous linewidth, are sufficiently narrow. The inhomogeneous and homogeneous linewidths are extremely sensitive to perturbations of the rare earth ions' local environment in the material; as a result, vastly different linewidths can be observed in nominally similar materials due to small differences in composition or growth conditions.[21,22] While the inhomogeneous linewidth provides a measure of the nanoscale uniformity of the crystal lattice throughout the macroscopic material, the homogeneous linewidth provides a measure of the perturbation dynamics and stability of the solid-state environment.[23] Consequently, the homogeneous linewidth can be significantly broadened by low levels of impurities with fluctuating electronic or nuclear spins or by low frequency vibrational modes in the lattice that are linked to local disorder in composition and structure. These effects are not manifest in conventional optical properties like fluorescence lifetimes, yet they give important information about impurities or structural defects present in the material. This is especially important in the case of ceramic materials to determine the role of grains boundaries, stress between grains, and possible residual impurities due to sintering aids used in the fabrication process.

In the work reported here, we study ceramic Y_2O_3 doped with trivalent europium. In bulk single crystals, Y_2O_3 can exhibit narrow homogeneous and inhomogeneous linewidths (see below), but crystal growth is difficult due to a very high melting temperature of ∼2400 °C. Since ceramic materials are produced by sintering nanocrystals at temperatures much lower than the bulk crystal's melting point, ceramic Y_2O_3 is of particular interest as a practical alternative to the single crystals. With this motivation, experiments were performed on a 10 mm diameter and 5.65 mm thick 0.1% (atomic) Eu^{3+} doped transparent ceramic sample of good optical quality

as shown in Fig. 1a inset.

The samples were synthesized from high purity (99.99%) Y_2O_3 and Eu_2O_3 powders, with particle sizes of 50 nm and 200 nm, respectively. The powders were mixed in ethanol for 15 hours by a ball milling process. The mixed slurry was dried on a hot plate to remove ethanol and then crushed into powders. The powders were uniaxially pressed with a modest pressure in a metal mold to form a pellet, which was then cold isostatically pressed at 98MPa. The pellets were pre-sintered in vacuum at 1500 °C for 3 hours, followed by hot isostatic pressing (HIP) at 1600 °C for 2 hours in Ar gas at a pressure of 147 MPa to achieve transparent ceramics. Inhomogeneous and homogeneous linewidth measurements were performed with the sample in a gas flow cryostat operated at controlled temperatures between 3 and 15 K. The laser source was a frequency-stabilized dye laser with a 1 MHz linewidth. Signals were detected by an amplified photodiode (transmission spectra) or an avalanche photodiode (photon echoes). Photon echoes were produced by focusing pulses of 1.5 μs to a 100 μm diameter spot in the ceramic. The laser power was 30 mW.

Fig. 1a presents the absorption spectrum of the Eu^{3+} $^7F_0 \rightarrow ^5D_0$ transition recorded at 15 K . This temperature was chosen to avoid hole burning effects due to optical pumping of ground state hyperfine levels. No significant dependence of absorption on polarization was observed as expected from the isotropic nature of the ceramic and the cubic structure (Ia3) of Y_2O_3. The line is centered at 580.88±0.05 nm (vacuum), within 10 GHz of the value reported for single crystals[21]. The full width at half maximum $\Gamma_{\rm inh}$ is 8.7 GHz. For the best bulk crystals with a comparable doping level, a similar $\Gamma_{\rm inh}$ value of 7.1 GHz has been observed.[21] In contrast, values as large as 90 GHz were found for a crystal grown using a mirror furnace[21]. The surprisingly narrow inhomogeneous linewidth in the ceramic material shows that the crystal field and residual lattice strain acting on the Eu^{3+} ions in the ceramic are comparable to those of the highest quality bulk crystals. This also indicates that the dopant is located within the crystalline grains and not in or near grain boundaries where large site distortions would be expected.

Homogeneous linewidths were measured by two pulse photon echo techniques. The decay of the photon echo intensity as a function of pulse delay was exponential (Fig. 1b), corresponding to a coherence lifetime T_2 of 5.4 μs and a homogeneous linewidth $\Gamma_h = 1/(\pi T_2)$ of 59 kHz at 3 K. In single crystals with similar doping levels, Γ_h at this temperature varies from 760 Hz to 62 kHz[21,24], depending on the growth method and the particular sample studied. The homogeneous linewidth in the ceramic is therefore within the range of values observed for single crystals, while showing a excess dephasing compared to the best samples. This can be analyzed by considering the different mechanisms that contribute to Γ_h[25]:

$$\Gamma_h = \Gamma_{\rm pop} + \Gamma_{\rm ion-ion} + \Gamma_{\rm ion-spin} + \Gamma_{\rm TLS} + \Gamma_{\rm phonon} \quad (1)$$

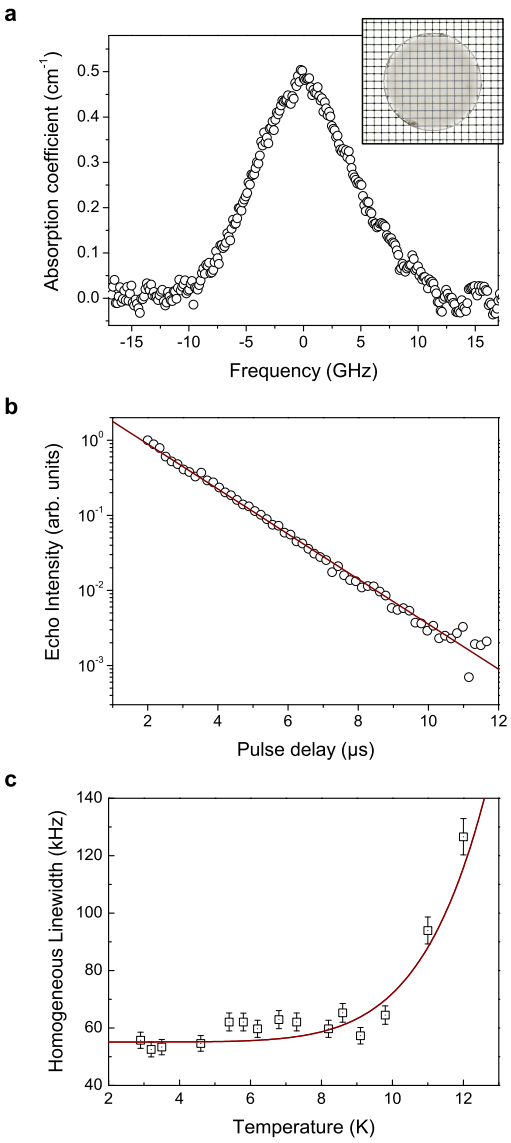

FIG. 1. Inhomogeneous and homogeneous linewidths of the Eu^{3+} $^7F_0 \rightarrow ^5D_0$ transition. **a**, Absorption spectrum (open circles) recorded at 15 K. Inset: image of the ceramic on a 1 mm grid. **b**, Two pulse photon echo intensity as a function of the pulse delay at 3 K (open circles) and exponential fit (solid line). **c**, Temperature dependence of homogeneous linewidth (Γ_h) obtained from two-pulse photon echo measurements (open squares) and fit using the Raman process expression (solid line).

where $\Gamma_{\rm pop}$ is the contribution from the excited-state population lifetime, $\Gamma_{\rm ion-ion}$ is the instantaneous spectral diffusion (ISD) contribution from changes in the local environment due to the optical excitation or population relaxation of other ions, $\Gamma_{\rm ion-spin}$ is the contribution

due to nuclear- and electron-spin fluctuations of the host lattice, $\Gamma_{\rm TLS}$ is the contribution due to dynamic fluctuations in nearly equivalent local lattice configurations, and $\Gamma_{\rm phonon}$ includes contributions from phonon scattering. The lifetime T_1 of the $^5D_0$ level in the ceramic is ∼1 ms, a value similar to that of the single crystal[21], corresponding to $\Gamma_{\rm pop} = 1/(2\pi T_1)$ ∼160 Hz. ISD is generally reduced at low excitation density and Eu^{3+} concentration. Since much narrower linewidths have been observed in single crystals with higher concentration under excitation conditions similar to those used here[24], it seems unlikely that the difference between our results and those reported in Ref. 21 and 24 could be attributed to ISD. The $\Gamma_{\rm ion-spin}$ broadening is often the ultimate limit for dephasing in rare earth doped single crystals, and the low magnetic moments of Y^{3+} and O^{2-} have allowed very narrow homogeneous linewidths to be observed in single crystals[24]. In the ceramic, additional impurities or defects that might be introduced during the synthesis process could have electronic or nuclear spins that contribute to $\Gamma_{\rm ion-spin}$. The $\Gamma_{\rm TLS}$ broadening is generally the most important effect in amorphous solids due to the many equivalent atom configurations that are possible in the disordered environment and the resulting fluctuations in the local environment due to tunneling between configurations with nearly equal energy, referred to as two-level systems (TLS). This process has also been observed at much lower levels in crystals with high strain or disorder[26,27], suggesting that it could be present in ceramic materials as well. Furthermore, from studies of glass ceramics it is known that Eu^{3+} ions in nanocrystals that are embedded in glass can experience dephasing due to long-range interactions with TLS in the glass host matrix[28], suggesting that interactions with grain boundaries could increase dephasing in ceramics with small grain sizes.

To further investigate the source of the observed dephasing, we measured the temperature dependence of the homogeneous linewidth Γ_h using photon echo measurements, as presented in Fig. 1c. Although $\Gamma_{\rm phonon}$, and therefore Γ_h, usually exhibits little dependence on temperature in the 1.5 - 4 K range for Eu^{3+}-doped single crystals, different behavior has sometimes been observed for Y_2O_3 single crystals grown by the laser-heated pedestal growth LHPG method[21]. In the LHPG crystals, Γ_h increased linearly with temperature over a temperature range from 1.5 to 10 K; moreover, the photon echo decays were slightly non-exponential. Both of those phenomena were attributed to glass-like configurational changes of the local structure of the host lattice due to the presence of TLS in the crystals. In the case of the LHPG single crystals, the source of TLS was attributed to structural defects. However, in our case, the broadening for the ceramic was well described by a T^7 temperature dependence that is characteristic of elastic Raman scattering of phonons[26,29] and corresponds to the expression: $\Gamma_h = \Gamma_0 + kT^7$ where T is the temperature. The best fit parameters are $\Gamma_0 = 55$ kHz and $k = 1.7 \times 10^{-6}$ kHz/K^7 (Fig. 1c., solid line). The broadening coefficient k for the ceramic agrees well with the value of 1.4×10^{-6} kHz/K^7 previously observed in high-quality single crystals[30]. Furthermore, analysis of the measured temperature dependence indicates that the maximum broadening due to TLS in the ceramic must be < 10 kHz/K to be consistent with the observed data. This level of TLS broadening is within the range observed for single crystals[21], demonstrating that the crystalline quality of the ceramic grains is comparable to Y_2O_3 single crystals. At 3 K, the maximum contribution of $\Gamma_{\rm TLS}$ in the ceramic would be ∼30 kHz, which is smaller than the observed Γ_h of 59 kHz. Together with the exponential echo decays, these observations suggest that any potential TLS broadening in the ceramic is too small to explain the measured homogeneous linewidth. Therefore, the Eu^{3+} dephasing most likely results from magnetic impurities (like transition metal or other rare earth ions) or defects inside the crystalline grains, perhaps in combination with a smaller contribution from disorder or impurities at the grain boundaries themselves. Reducing these contributions by optimizing synthesis and starting material purity seems to be the best way to increase coherence lifetimes. Indeed, techniques like zero first order Zeeman shift[31,32], which rely on external control fields to decouple rare earth ions from environment, may be difficult to apply because of the isotropic nature of the ceramic.

The analysis of the homogeneous broadening is consistent with the narrow $^5D_0 \rightarrow ^7F_0$ inhomogeneous linewidth and again supports the conclusion that Eu^{3+} ions do not segregate at the grain boundaries. To confirm this last conclusion, we examined the ceramic microstructure by confocal luminescence[33], using the $^5D_0 \rightarrow ^7F_2$ transition intensity to map the spatial distribution of Eu^{3+} ions (Fig. 2a). Excitation was provided by an Ar^+ laser at 488 nm focused into the sample by a microscope objective (100x magnification) to a spot size smaller than 1 μm. The photoluminescence was collected in backscattering geometry and focused into a multi-mode fiber connected to a spectrometer equipped with a CCD camera. The sample was placed on a 2-axis XY motorized stage with 0.1 μm spatial resolution, thus precise positioning of the sample under the laser spot was achieved. The corresponding image (Fig. 2 b) did not reveal any significant variations. This result indicates that no segregation of Eu^{3+} ions towards grain boundaries occurred. To reveal grains and grain boundaries, the ceramic was then etched in nitric acid for 5 min at 100 °C. Optical images (Fig. 2 (c)) show a mean grain size of ∼50 μm and correspond closely to those obtained by confocal luminescence (Fig. 2 d). The large grain size and the absence of Eu^{3+} segregation is consistent with the conclusion drawn from inhomogeneous and homogeneous linewidths.

In conclusion, we report for the first time, to our knowledge, high-resolution measurements of the inhomogeneous and homogeneous linewidths in a transparent ceramic at low temperatures. The 8.7 GHz inhomogeneous linewidth is close to that of single crystals, as is

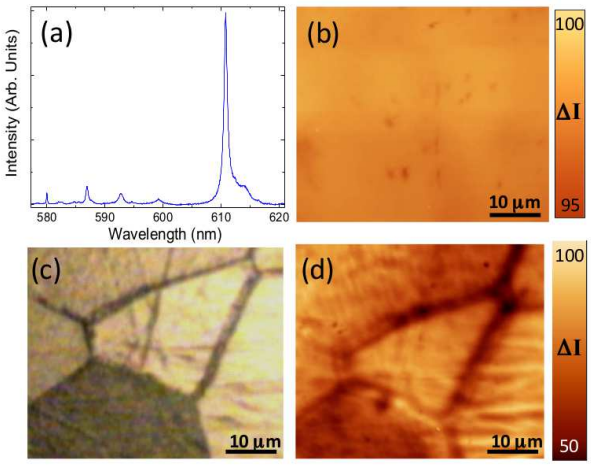

FIG. 2. **a**, Luminescence spectrum obtained by confocal microscopy at room temperature on the ceramic surface. The $^5D_0 \rightarrow ^7F_2$ transition occurs at 611 nm and its intensity was used to map Eu^{3+} spatial distribution. **b,d**, Confocal fluorescence map of the ceramic surface obtained before (**b**) or after (**d**) chemical etching. The color scale on the right gives the luminescence intensity variations. **c**, Optical microscopy image of the ceramic surface after chemical etching.

the 59 kHz homogeneous linewidth at 3 K ($T_2 = 5.4$ μs). The photon echo decays are exponential and the homogeneous linewidth dependence on temperature is typical of single crystals, further showing the high crystalline quality of the ceramic grains and the low influence of grain boundaries on Eu^{3+} dephasing. The observation of relatively large grain size (50 μm) and the absence of Eu^{3+} segregation in the grains indicate that the majority of Eu^{3+} ions in the ceramic experience an environment comparable to a single crystal. Additional dephasing observed in the ceramic is attributed to magnetic impurities or defects introduced during the synthesis process. Together, all of these results show that it is possible to study transparent ceramics by techniques that probe the nanoscale dynamics and structure of the rare earth ion environment. Moreover, the specific results obtained here suggest that ceramic materials can be competitive with single crystals for applications in quantum information and spectral hole burning devices, beyond their current applications in lasers and scintillators.

ACKNOWLEDGEMENTS

This work was supported by National Science Foundation under award No. PHY-1212462, the European Union FP7 project QuRep (247743), the Spanish Ministry of Economy and Competitiveness (MAT2010-17443) and Comunidad de Madrid (S-2009/MAT-1756).

* philippe-goldner@chimie-paristech.fr

[1] A. Ikesue and Y. L. Aung, Nat. Photon. **2**, 721 (2008).
[2] V. Lupei, A. Lupei, and A. Ikesue, Optical Materials **30**, 1781 (2008).
[3] A. Fukabori, T. Yanagida, J. Pejchal, S. Maeo, Y. Yokota, A. Yoshikawa, T. Ikegami, F. Moretti, and K. Kamada, J. Appl. Phys. **107**, 073501 (2010).
[4] E. Zych, C. Brecher, A. Wojtowicz, and H. Lingertat, J. Lumin. **75**, 193 (1997).
[5] A. Lempicki, C. Brecher, P. Szupryczynski, H. Lingertat, V. Nagarkar, S. Tipnis, and S. Miller, Nucl. Instrum. Methods Phys. Res. A **488**, 579 (2002).
[6] T. Yanagida, Y. Fujimoto, Y. Yokota, A. Yoshikawa, S. Kuretake, Y. Kintaka, N. Tanaka, K. Kageyama, and V. Chani, Opt. Mat. **34**, 414 (2011).
[7] A. Ikesue, T. Kinoshita, K. Kamata, and K. Yoshida, J. Am. Ceram. Soc. **78**, 1033 (1995).
[8] I. Shoji, S. Kurimura, Y. Sato, T. Taira, A. Ikesue, and K. Yoshida, Appl. Phys. Lett. **77**, 939 (2000).
[9] B. Zhou, Z. Wei, Y. Zou, Y. Zhang, X. Zhong, G. L. Bourdet, and J. Wang, Opt. Lett. **35**, 288 (2010).
[10] G. Q. Xie, D. Y. Tang, L. M. Zhao, L. J. Qian, and K. Ueda, Opt. Lett. **32**, 2741 (2007).
[11] T. Sanamyan, M. Kanskar, Y. Xiao, D. Kedlaya, and M. Dubinskii, Opt. Express **19**, A1082 (2011).
[12] W. Tittel, M. Afzelius, T. Chanelière, R. Cone, S. Kröll, S. Moiseev, and M. Sellars, Laser & Photon. Rev. **4**, 244 (2010).
[13] C. Clausen, I. Usmani, F. Bussières, N. Sangouard, M. Afzelius, H. de Riedmatten, and N. Gisin, Nature **469**, 508 (2011).
[14] E. Saglamyurek, N. Sinclair, J. Jin, J. A. Slater, D. Oblak, F. Bussières, M. George, R. Ricken, W. Sohler, and W. Tittel, Nature **469**, 512 (2011).
[15] I. Usmani, C. Clausen, F. Bussieres, N. Sangouard, M. Afzelius, and N. Gisin, Nat. Photon. **6**, 234 (2012).
[16] M. P. Hedges, J. J. Longdell, Y. Li, and M. J. Sellars, Nature **465**, 1052 (2010).
[17] J.-L. Le Gouët, F. Bretenaker, and I. Lorgeré, in *Advances in Atomic Molecular and Optical Physics*, Vol. 54 (Academic Press, 2006) pp. 549–613.
[18] Y. Li, P. Hemmer, C. Kim, H. Zhang, and L. V. Wang, Opt. Express **16**, 14862 (2008).
[19] P. B. Sellin, N. M. Strickland, J. L. Carlsten, and R. L. Cone, Opt. Lett. **24**, 1038 (1999).
[20] M. J. Thorpe, L. Rippe, T. M. Fortier, M. S. Kirchner, and T. Rosenband, Nat. Photon. **5**, 688 (2011).
[21] G. P. Flinn, K. W. Jang, J. Ganem, M. L. Jones, R. S. Meltzer, and R. M. Macfarlane, Phys. Rev. B **49**, 5821 (1994).
[22] T. Okuno and T. Suemoto, Phys. Rev. B **59**, 9078 (1999).
[23] R. M. Macfarlane, J. Lumin. **100**, 1 (2002).
[24] R. Macfarlane and R. Shelby, Optics Communications **39**, 169 (1981).
[25] R. M. Macfarlane and R. M. Shelby, in *Spectroscopy of Solids Containing Rare Earth Ions*, edited by A. A. Kaplyanskii and R. M. Macfarlane (Amsterdam: North-Holland, 1987) p. 51.
[26] R. M. Macfarlane, F. Könz, Y. Sun, and R. L. Cone, J. Lumin. **86**, 311 (2000).
[27] S. K. Watson, Phys. Rev. Lett. **75**, 1965 (1995).
[28] R. S. Meltzer, W. M. Yen, H. Zheng, S. P. Feofilov, M. J. Dejneka, B. M. Tissue, and H. B. Yuan, Phys. Rev. B **64**, 100201 (2001).
[29] D. E. McCumber and M. D. Sturge, J. Appl. Phys. **34**, 1682 (1963).
[30] W. R. Babbitt, A. Lezama, and T. W. Mossberg, Phys. Rev. B **39**, 1987 (1989).
[31] E. Fraval, M.-J. Sellars, and J.-J. Longdell, Phys. Rev. Lett. **92**, 077601 (2004).
[32] M. Lovric, P. Glasenapp, D. Suter, B. Tumino, A. Ferrier, P. Goldner, M. Sabooni, L. Rippe, and S. Kröll, Phys. Rev. B **84**, 104417 (2011).
[33] M. O. Ramirez, J. Wisdom, H. Li, Y. L. Aung, J. Stitt, G. L. Messing, V. Dierolf, Z. Liu, A. Ikesue, R. L. Byer, and V. Gopalan, Opt. Express **16**, 5965 (2008).